

# pH-Dependent surface-enhanced resonance Raman scattering of yeast *iso-1*-cytochrome *c* adsorbed on silver nanoparticle surfaces under denaturing conditions at pH < 3

So Yeong Lee<sup>1</sup>, Sang-Woo Joo<sup>2,\*</sup>, Seonghoon Lee<sup>3</sup> & Manho Lim<sup>4,\*</sup>

<sup>1</sup>Department of Pharmacology, College of Veterinary Medicine, Seoul National University, Seoul 151-742, <sup>2</sup>Department of Chemistry, Soongsil University, Seoul 156-743, <sup>3</sup>School of Chemistry and Molecular Engineering, Seoul National University, Seoul 151-747,

<sup>4</sup>Department of Chemistry and Chemistry Institute for Functional Materials, Pusan National University, Busan 609-735, Korea

**We measured the pH-induced spectral changes of yeast *iso-1*-cytochrome *c* on silver nanoparticle surfaces using surface-enhanced resonance Raman scattering (SERRS) at 457.9 nm. At a pH of ~3, the Met80 ligand in yeast *iso-1*-cytochrome *c* is assumed to dissociate, leading to a marked conformational change as evidenced by the vibrational spectral shifts. The Soret band at ~410 nm in the UV-Vis spectrum shifted to ~396 nm at pH ~3, indicating a transition from a low spin state to a high spin state from a weak interaction with a water molecule. Thus, SERRS spectroscopy can measure the pH-induced denaturalization of cyt *c* adsorbed on metal nanoparticle surfaces at a lower concentration with a better sensitivity than ordinary resonance Raman spectroscopy. [BMB reports 2009; 42(4): 223-226]**

## INTRODUCTION

Conformational changes in proteins are important in understanding biological interactions (1, 2). Cytochrome *c* regulates mitochondrial electron transfer activity, apoptosis, and biological activity (1-6). A conformational transition between  $\beta$ -sheet aggregation and disordered structure occurs in cytochrome *c* (7). In the ferric form, the heme iron is axially coordinated by two internal ligands, histidine and methionine, leading to a six-coordinated low spin (6cLS) configuration (8).

Yeast *iso-1*-cytochrome *c* isolated from *Saccharomyces cerevisiae* is a soluble 12.6 kDa monoheme protein (9, 10). In the native state of yeast *iso-1*-cytochrome *c*, the heme group in the protein is covalently attached to the His 18 and Met 80 residue. During protein unfolding, the methionine ligand is dissociated

from the heme and replaced by the other histidine group or water molecules, leading to a high spin state (9-11). Yeast *iso-1*-cytochrome *c* can be covalently bound to the metal surface by a thiol group in the cysteine residue (12-14). Yeast *iso-1*-cytochrome *c* bound on gold nanoparticles can be a colorimetric sensor because it unfolds at low pH and refolds at high pH 8 (15).

Silver nanoparticles have attracted much attention in the past decade due to their stability and optical properties (16). Biological applications focus on the effect of size, shape, biocompatibility, uptake, and sub-cellular distribution of silver nanoparticles. Colloidal silver nanoparticles are popular platforms for surface enhanced Raman scattering (SERS) (17).

SERS is an ultra-sensitive spectroscopic tool for interface studies as chemical sensors in biophysical chemistry (18). Chemically-specific information is provided by unique vibrational modes of target adsorbates, which depends on the metal substrates (19-23). However, the detailed adsorption characteristics on metal surfaces have not been fully clarified. In this study, we examined the adsorption behaviors of yeast *iso-1*-cytochrome *c* on Ag nanoparticle surfaces using SERS to better understand the pH-induced conformational changes on metal surfaces.

## RESULTS

### UV-Vis absorbance spectra

Fig. 1A shows the pH-induced UV-Vis absorbance spectra of  $\sim 10^{-5}$  M yeast *iso-1*-cytochrome *c* in aqueous solution. The Soret and Q transitions bands were found at 410 and 523 ~ 550 nm, respectively. The arrows indicate the excitation wavelengths at 457.9 nm for Ag SERRS experiments. Our excitation wavelength lies between the Soret and Q band. Fig. 1B shows UV-Vis absorbance spectra of citrate-reduced Ag nanoparticles. The excitation wavelengths at 457.9 nm should lie close to the surface plasmon resonance band of the silver nanoparticles, which may produce a strong enhancement in the SERRS experiments.

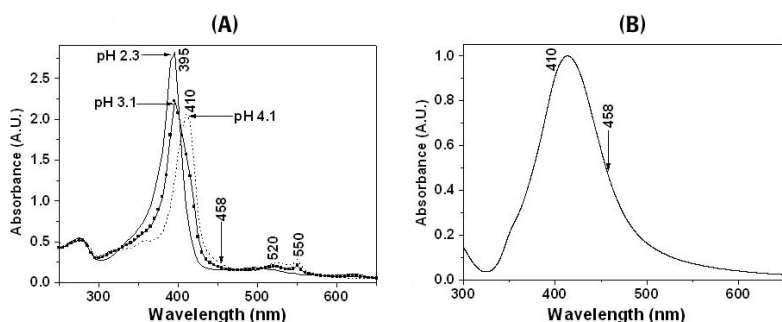
### Resonance Raman spectra of yeast *iso-1*-cytochrome *c*

Fig. 2 shows Raman spectra of yeast *iso-1*-cytochrome *c* in the

\*Corresponding author. Manho Lim, Tel: 82-51-510-2243; Fax: 82-51-5167421; E-mail: mhl@pusan.ac.kr; Sang-Woo Joo, Tel: 82-2-820-0434; Fax: 82-2-8200434; E-mail: sjoo@ssu.ac.kr

Received 6 November 2008, Accepted 16 December 2008

**Keywords:** Ag nanoparticles, pH change, SERRS, UV-Vis absorption, Yeast *iso-1*-cytochrome *c*



**Fig. 1.** (A) pH-induced UV-Vis absorbance spectra of  $\sim 10^{-3}$  M yeast *iso-1*-cytochrome c in aqueous solution. The Soret and Q bands were found at 410 and 523–550 nm, respectively. Arrows indicate the excitation wavelengths at 457.9 nm for Ag SERRS experiments. (B) UV-Vis absorbance spectral change in citrate reduced-Ag colloidal nanoparticles. The arrows indicate the excitation wavelengths at 457.9 nm for Ag SERRS experiments.

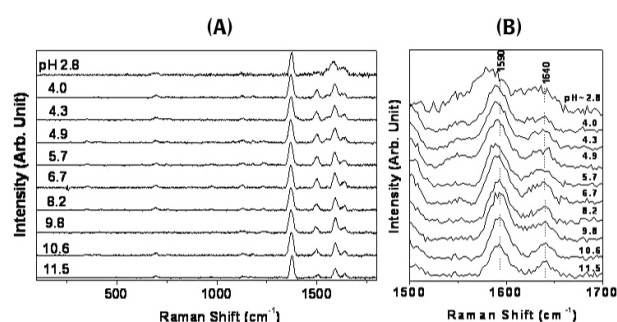


**Fig. 2.** (A) Resonance Raman (RR) spectra of  $\sim 10^{-3}$  M yeast *iso-1*-cytochrome c in distilled water upon irradiation using 457.9 nm at pH 2.8–11.5 in the spectral region between 300 and 1,800  $\text{cm}^{-1}$ . (B) An expanded view of RR spectra of  $\sim 10^{-3}$  M yeast *iso-1*-cytochrome c between 1,500 and 1,700  $\text{cm}^{-1}$ .

spectral region between 300 and 1,800  $\text{cm}^{-1}$  at the excitation wavelength of 457.9 nm. The spectral features appeared to depend on the excitation wavelengths of 457.9, 514.5, and 632.8 nm, presumably due to the different resonance enhancements for a specific vibrational band (data not shown; 11). Fig. 2 also compares resonance Raman (RR) spectra of  $\sim 10^{-3}$  M yeast *iso-1*-cytochrome c at pH values of 2.8–11.5 in aqueous solutions. We analyzed the Raman spectrum referring to earlier vibrational assignments described in the literature (11, 24, 25). In the RR spectrum, the spectral positions did not change significantly by varying pH above pH 3. An expanded view for the  $\nu_{19}$  (or  $\nu_{11}$ ) and  $\nu_{10}$  bands in the 1,500–1,700  $\text{cm}^{-1}$  region is reproduced in Fig. 2B for a better comparison.

### Surface-enhanced resonance Raman spectra of yeast *iso-1*-cytochrome c on Ag nanoparticle surfaces

Fig. 3 compares surface-enhanced resonance Raman scattering (SERRS) spectra of  $\sim 10^{-4}$  M yeast *iso-1*-cytochrome c on Ag nanoparticles at pH values of 2.3–11.3 in aqueous solutions. The SERRS spectra at  $\sim 10^{-4}$  M in Fig. 3 appeared to be more enhanced than those at  $\sim 10^{-3}$  M in the resonance Raman (RR) spectrum of Fig. 2. The bandwidths were broadened after adsorption on Ag, indicating an interaction between Ag nanoparticles and yeast *iso-1*-cytochrome c. At neutral alkaline pH

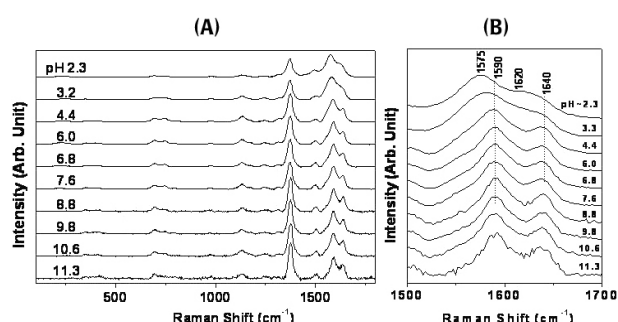


**Fig. 3.** (A) SERRS spectra of  $\sim 10^{-4}$  M yeast *iso-1*-cytochrome c on Ag nanoparticle surfaces upon irradiation using 457.9 nm at pH 2.3–11.3 in the spectral region between 300 and 1,800  $\text{cm}^{-1}$ . (B) An expanded view of SERRS spectra of  $\sim 10^{-4}$  M yeast *iso-1*-cytochrome c region between 1,500 and 1,700  $\text{cm}^{-1}$ .

values, the marker bands  $\nu_4$ ,  $\nu_3$ ,  $\nu_{19}$  (or  $\nu_{11}$ ), and  $\nu_{10}$  were observed at 1,375, 1,498, 1,592, and 1,640  $\text{cm}^{-1}$ , respectively. These bands were red-shifted to 1,372, 1,489, 1,571, and 1,620  $\text{cm}^{-1}$ , respectively, by lowering pH below  $\sim 3$ , suggesting a structural change (Table 1). An expanded view of the  $\nu_{19}$  (or  $\nu_{11}$ ) and  $\nu_{10}$  bands in the 1,500–1,700  $\text{cm}^{-1}$  region is reproduced in Fig. 3B for a better comparison.

The Raman enhancements on Au nanoparticles were smaller than on Ag nanoparticles (data not shown). Raman spectra on Au nanoparticles were examined at pH values of 2.8–10.5. The marker bands  $\nu_{11}$  and  $\nu_{10}$  were observed at 1,550 and 1,625  $\text{cm}^{-1}$ , respectively. These bands were red-shifted to 1,545 and 1,610  $\text{cm}^{-1}$ , respectively, by lowering pH. Au nanoparticles showed a conformational change at pH  $\sim 6$ , higher than Ag nanoparticles at pH  $\sim 3$  (15), suggesting greater stability when the protein is adsorbed to Ag nanoparticles (26). As nanoparticles are added to yeast *iso-1*-cytochrome c solution, the peak starts to shift at higher pH, indicating protein destabilization. Thus, SERRS and SERS can measure the pH-induced conformational changes of yeast *iso-1*-cytochrome c adsorbed on metal nanoparticle surfaces at a lower concentration with a better sensitivity.

**Table 1.** Spectral data and vibrational assignments for yeast iso-1-cytochrome

RR <sup>a</sup>	Ag SERRS at each pH										Tentative assignment <sup>b</sup>	
	2.3	3.2	4.4	6.0	6.8	7.6	8.8	9.8	10.6	11.3		
354	234	241	236	228	231	226						Ag-S
	345	349	349	352	348	350	349	352	349	346		v <sub>51</sub> δ (C <sub>β</sub> -C <sub>1</sub> ) <sub>asym</sub>
696	692	695	696	696	695	693	694	694	695	693		v <sub>4</sub> δ (C <sub>β</sub> -C <sub>c</sub> -C <sub>d</sub> )
	753	754	746	747	746	747	745	741	745	744		v (C-S)
1,133	978	977	973	975	975	975	968	968	971	978		v <sub>15</sub> (pyr breathing)
	1,132	1,132	1,133	1,133	1,128	1,130	1,133	1,129	1,132	1,133		δ <sub>46</sub> (pyr deform) <sub>asym</sub>
1,181												v <sub>22</sub> (pyr half-ring) <sub>asym</sub>
	1,235	1,243	1,245	1,246	1,245	1,243	1,247	1,252	1,246	1,249		v <sub>30</sub> (pyr half-ring) <sub>sym</sub>
1,370												δ <sub>13</sub> (C <sub>m</sub> -H)
	1,372	1,372	1,374	1,374	1,375	1,373	1,372	1,375	1,375	1,377	1,375	δ <sub>22</sub> (C <sub>m</sub> -H)
1,502	1,493	1,500	1,501	1,500	1,499	1,499	1,502	1,503	1,503	1,507		v <sub>4</sub> (pyr half-ring) <sub>sym</sub>
	1,592	1,577	1,580	1,589	1,591	1,591	1,591	1,590	1,591	1,593		v <sub>3</sub> v (C <sub>α</sub> -C <sub>m</sub> ) <sub>sym</sub>
1,638												v <sub>11</sub> v (C-C)
	1,618	1,620	1,637	1,638	1,638	1,638	1,640	1,638	1,638	1,635		v <sub>19</sub> v (C <sub>α</sub> -C <sub>m</sub> ) <sub>asym</sub>
												v <sub>10</sub> v (C <sub>α</sub> -C <sub>m</sub> ) <sub>asym</sub>

<sup>a</sup>Resonance Raman measurements at pH ~5.7. <sup>b</sup>Based on refs. 11,24, and 25.

## DISCUSSION

The pH-induced structural changes of yeast iso-1-cytochrome c on silver nanoparticle surfaces were investigated using SERRS. At pH below ~3, the methionine or histidine ligand in yeast iso-1-cytochrome c dissociates, causing a marked change in the conformation of the molecule. At neutral alkaline potentials, the oxidation marker bands v<sub>4</sub>, v<sub>3</sub>, v<sub>19</sub> (or v<sub>11</sub>), and v<sub>10</sub> were observed at 1,375, 1,498, 1,592, and 1,640 cm<sup>-1</sup>, respectively, indicating yeast iso-1-cytochrome c with a heme Fe<sup>3+</sup> in a low-spin state. These bands were red shifted to 1,372, 1,489, 1,571, and 1,620 cm<sup>-1</sup>, respectively, by lowering pH below 3, suggesting a rupture of the Met80 and His18 ligand of yeast iso-1-cytochrome with a high-spin state. This structural transition occurs at a pH of ~3 for silver nanoparticles.

## MATERIALS AND METHODS

### Sample preparation

Yeast iso-1-cytochrome c from *Saccharomyces cerevisiae* was purchased from Sigma and used without further purification. Colloidal silver nanoparticles were prepared according to the procedures reported in the literature, wherein sodium citrate was used as a reducing agent (27). A portion of AgNO<sub>3</sub> (~90 mg) was dissolved in ~500 mL of distilled water, brought to boiling, and a solution of ~1% sodium citrate (10 mL) was added and boiled for ca. 1 h. All chemicals used were reagent-grade unless otherwise specified. Triply-distilled water of resistivity greater than 18.0 MΩ · cm was used in making aqueous solutions.

### Instrumental measurements

Raman spectra were obtained using a Renishaw Raman con-

focal system Model 1,000 spectrometer equipped with an integral microscope (Leica DM LM). The 457.9 irradiation was from a 50 mW air-cooled Ar ion laser (Melles Griot Model LAP 431) (28). The 632.8 nm radiation was from and a 35 mW air-cooled He-Ne laser (Melles Griot Model 25 LHP 928) with a plasma line rejection filter used as the excitation sources for the SERS experiments on Ag nanoparticles. UV-Vis absorbance spectra were obtained using a Mecasys Optizen 3220 spectrophotometer. The pH values of Ag nanoparticle solutions were measured using a Thermoelectron Orion 3 star bench top pH meter (29). pH control was performed by the addition of 1 M NaOH or 1 M HCl stock solutions. For low pH measurements, the 1 M HCl stock solution was diluted to 1-50 mM. A microdroplet of each HCl solution was added to the cytochrome c-adsorbed Ag nanoparticle solution, in a volume of ~300 μL, to lower the pH values. The pH was similarly increased by NaOH.

### Acknowledgments

Sang-Woo Joo would like to thank Mr. Hyung-Woo Choi for helping with experiments. This work was supported by the Korea Research Foundation Grant funded by the Korean Government (MOEHRD) (KRF-2007-314-C00146). This work was supported by the Soongsil University Research Fund. This research was supported by the Nano R&D program through the Korea Science and Engineering Foundation funded by the Ministry of Education, Science and Technology (2008-04308).

## REFERENCES

- Harper, S. M., Neil, L. C. and Gardner, K. H. (2003) Structural basis of a phototropin light switch. *Science* **301**, 1541-1544.

- Green, D. R. and Reed, J. C. (1998) Mitochondria and apoptosis. *Science* **281**, 1309-1312.
- Seo, Y. W., Park, S. Y., Yun, C. W. and Kim, T. H. (2006) Differential efflux of mitochondrial endonuclease G by hNoxa and tBid. *JBMB* **39**, 556-559.
- Kim, N. H. and Kang, J. H. (2006) Oxidative damage of DNA induced by the cytochrome c and hydrogen peroxide system. *JBMB* **39**, 452-456.
- Park, Y. J., Yoo, C. B., Choi, S. Y. and Lee, H. B. (2006) Purifications and characterizations of a ferredoxin and its related 2-oxoacid: ferredoxin oxidoreductase from the hyperthermophilic archaeon, *Sulfolobus solfataricus* P1. *JBMB* **39**, 46-54.
- Park, J. H. and Kim, T. H. (2005) Release of cytochrome c from isolated mitochondria by etoposide. *JBMB* **38**, 619-623.
- Balakrishnan, G., Hu, Y., Oyerinde, O. F., Su, J., Grove, J. T. and Spiro, T. G. (2007) Conformational switch to  $\beta$ -sheet structure in cytochrome c leads to heme exposure. Implications for cardiolipin peroxidation and apoptosis. *J. Am. Chem. Soc.* **129**, 504-505.
- Rivas, L., Murgida, D. H. and Hildebrandt, P. (2001) Surface-enhanced resonance Raman study of cytochrome c from *Methylophilus methylotrophus*. *J. Mol. Struct.* **565-566**, 193-196.
- Godbole, S. and Bowler, B. E. (1999) Effect of pH on formation of a natively-like intermediate on the unfolding pathway of a Lys 73 $\rightarrow$ His variant of yeast iso-1-cytochrome c. *Biochemistry* **38**, 487-495.
- Godbole, S., Hammack, B. and Bowler, B. E. (2000) Measuring denatured state energetics: deviations from random coil behavior and implications for the folding of iso-1-cytochrome c. *J. Mol. Biol.* **296**, 217-228.
- Siebert, F. and Hildebrandt, P. (2008) *Vibrational Spectroscopy in Life Science*, Wiley-VCH, Verlag.
- Schweitzer-Stenner, R., Huang, Q., Hagarman, A., Laberge, M. and Wallace, C. J. A. (2007) Static normal coordinate deformations of the heme group in mutants of ferrocycytochrome c from *Saccaromyces cerevisiae* probed by resonance Raman spectroscopy. *J. Phys. Chem. B* **111**, 6527-6533.
- Zheng, J., Zho, Q., Zho, Y., Lu, T., Cotton, T. M. and Chumanov, G. (2002) Surface-enhanced resonance Raman spectroscopic study of yeast iso-1-cytochrome c and its mutant. *J. Electroanal. Chem.* **530**, 75-81.
- Blouin, C., Guillemette, J. G. and Wallace, C. J. A. (2001) Resolving the individual components of a pH-induced conformational change. *Biophys. J.* **81**, 2331-2338.
- Chah, S., Hammond, M. R. and Zare, R. N. (2005) Gold nanoparticles as a colorimetric sensor for protein conformational changes. *Chem. & Bio.* **12**, 323.
- Shipway, A. N., Katz, E. and Willner, I. (2000) Nanoparticle arrays on surfaces for electronic, optical, and sensor applications. *Chem. Phys. Chem.* **1**, 18-52.
- Patra, H. K., Banerjee, S., Chaudhuri, U., Lahiri, P. and Dasgupta, A. (2007) Cell selective response to gold nanoparticles. *Nanomedicine* **3**, 111.
- Schatz, G. C. and van Duyne, R. P. (2002) Electromagnetic mechanism of surface-enhanced Raman spectroscopy; in *Handbook of Vibrational Spectroscopy*, Chalmers, J. M. and Griffiths, P. R. (eds.), pp. 759-774, John Wiley & Sons, New York, USA.
- Bae, S. J., Lee, C. R., Choi, I. S., Hwang, C. S., Gong, M. S., Kim, K. and Joo, S. W. (2002) Adsorption of 4-biphenylisocyanide on gold and silver nanoparticle surfaces: surface-enhanced Raman scattering study. *J. Phys. Chem. B* **106**, 7076-7080.
- Lee, C. R., Bae, S. J., Gong, M. S., Kim, K. and Joo, S. W. (2002) Surface-enhanced Raman scattering of 4,4'-dicyanobiphenyl on silver and gold nanoparticle surfaces. *J. Raman Spectrosc.* **33**, 429-433.
- Joo, S. W., Chung, T. D., Jang, W., Gong, M. S., Geum, N. and Kim, K. (2002) Surface-enhanced Raman scattering of 4-cyanobiphenyl on gold and silver nanoparticle surfaces. *Langmuir* **18**, 8813-8816.
- Cho, K. H., Choo, J. and Joo, S. W. (2005) Surface enhanced Raman scattering and density functional theory calculation of uracil on gold and silver nanoparticle surfaces. *Spectrochim. Acta. A* **61**, 1141-1145.
- Cho, K. H., Choo, J. and Joo, S. W. (2005) Tautomerism of thymine on gold and silver nanoparticles surfaces: surface enhanced Raman scattering and density functional calculation study. *J. Mol. Struct.* **738**, 9-14.
- Dick, L. A., Haes, A. J. and van Duyne, R. P. (2000) Distance and orientation dependence of heterogeneous electron transfer: a surface-enhanced resonance Raman scattering study of cytochrome c bound to carboxylic acid terminated alkanethiols adsorbed on silver electrodes. *J. Phys. Chem. B* **104**, 11752-11762.
- Sage, J. T., Morikis, D. and Champion, P. M. (1991) Spectroscopic studies of myoglobin at low pH: heme structure and ligation. *Biochemistry* **30**, 1227-1237.
- Oellerich, S., Wackerbarth, H. and Hildebrandt, P. (2002) Spectroscopic characterization of nonnative conformational states of cytochrome c. *J. Phys. Chem. B* **106**, 6566-6580.
- Lee, P. C. and Meisel, D. (1982) Adsorption and surface-enhanced Raman dyes on silver and gold sols. *J. Phys. Chem.* **86**, 3391-3395.
- Lim, J. K. and Joo, S. W. (2007) Excitation-wavelength-dependent charge transfer resonance of bipyridines on silver nanoparticles: surface-enhanced Raman scattering study. *Surf. Interf. Anal.* **39**, 684-690.
- Lim, J. K. and Joo, S. W. (2006) Gold Nanoparticle-based pH sensor in highly alkaline region at pH > 11: surface-enhanced Raman scattering study. *Appl. Spectrosc.* **60**, 847-852.